Multi-objective design of reverse osmosis plants integrated with solar Rankine cycles and thermal energy storage

Ekaterina Antipova[a], Dieter Boer[b,*], Luisa F. Cabeza[c], Gonzalo Guillén-Gosálbez[a], Laureano Jiménez[a]

[a]*Departament d 'Enginyeria Química (EQ), Universitat Rovira i Virgili (URV),Campus Sescelades, Avinguda Països Catalans, 26, 43007 Tarragona, Spain*
[b]*Departament d 'Enginyeria Mecànica (EQ), Universitat Rovira i Virgili (URV),Campus Sescelades, Avinguda Països Catalans, 26, 43007 Tarragona, Spain*
[c]*Edifici CREA, Universitat de Lleida, Pere de Cabrera s/n, 25001-Lleida, Spain*

Abstract

This paper addresses the optimal design of desalination plants that integrate reverse osmosis, a Rankine cycle, parabolic trough solar collectors and thermal energy storage (TES). A multi-objective mixed-integer nonlinear programming model (MINLP) is developed to model such an integrated system and optimize its design and operating conditions according to economic and environmental metrics. The model considers the simultaneous minimization of cost and environmental impact given a specific water demand to be fulfilled. The environmental performance is quantified via life cycle assessment (LCA) principles. Particularly, the CML 2001 methodology, a widely used LCA-based framework, is used to assess the impact, enabling the identification of the main sources of damage across the entire life cycle of the plant. The capabilities of our method are illustrated through its application to a case study considering weather data in Tarragona (Spain). We show that coupling seawater desalination with solar collectors and thermal energy storage leads to significant environmental savings at a marginal increase in cost.

Keywords: desalination, multi-objective optimization, life cycle assessment (LCA), solar energy, modelling, thermal energy storage (TES), mixed-integer non linear programming (MINLP)

1. Introduction

Reverse Osmosis (RO) is currently the most popular technique to obtain fresh water from saline one [1]. The actual trend in environmental policy is favouring the adoption of sustainable technologies in standard industrial processes. One technology that implements these ideas is the integration of solar power with standard desalination processes. This technology has been already investigated at a small scale in remote areas. Its implementation at a larger scale, however, poses some difficulties and challenges that still merit further attention and research. This task is of great current interest, as desalination at large scale can result in both lower unitary production cost of water and lower environmental impact [2].

The performance of the combined system (RO with solar collectors) can be further improved through its integration with thermal energy storage (TES). This technology allows storing the excess of energy produced in the collectors during periods with high irradiance. The stored energy can then be used in later periods with solar energy intermittency or during the nights. TES leads to significant environmental benefits such as reductions in fossil fuels consumption and CO_2 emissions, thereby mitigating climate change [3]. Furthermore, TES can improve the economic performance and capacity factor of the whole system,thereby increasing its flexibility [4–6].

The design of solar desalination facilities aims to identify the best system configuration and operating conditions given a water demand to be fulfilled, environmental, and cost data [7]. The environmental impact of the process depends on the configuration of the system and operation conditions. The design task requires the evaluation of a very large number of feasible (and potentially optimal) process alternatives, from which the

*Correspondence concerning this article should be addressed to Dieter Boer at Dieter.Boer@urv.cat
Email addresses: ekaterina.antipova@urv.cat (Ekaterina Antipova), Dieter.Boer@urv.cat (Dieter Boer), lcabeza@diei.udl.cat (Luisa F. Cabeza), gonzalo.guillen@urv.cat (Gonzalo Guillén-Gosálbez), laureano.jimenez@urv.cat (Laureano Jiménez)

best in terms of economic and environmental performance are finally identified. Optimization tools provide a systematic framework to accomplish this task. Different optimization approaches have been proposed in the literature for desalination processes. Despite being widely used nowadays, reverse osmosis has the drawback of consuming huge amounts of electricity for operating the high pressure pumps. Hence, a large body of literature has concentrated on improving the membrane performance to reduce this energy consumption [8, 9]. A non-linear membrane model was proposed by Bartman et al. in order to identify the membrane operating conditions that minimize the energy consumption [8]. Kaghazhi et al. elaborated a model of a RO unit which allows to find the optimal membrane working conditions (e.g., pressure, concentrations, feed flow rate, etc.) in order to ensure a minimum production cost [9]. None of these studies considered the integration of the RO plant with solar energy. Other optimization works addressed the integration of renewable energy sources with RO. Different models were suggested to find process configurations with minimum production cost [10–12]. Ben Bacha et al. examined the problem of energy intermittency. Other authors studied multi-effect humidification assisted by solar collectors to treat the brackish water, and various storage tanks to ensure continuous energy supply [13].

Several investigations have been focused on the minimization of the environmental impact of different desalination technologies. Two major issues are nowadays in the limelight. The first concerns the greenhouse gas (GHG) emissions. The use of renewable energy sources can substantially reduce the environmental impact related to GHG emissions [14]. Raluy et al. reported that by integrating renewable energy sources in industrial RO plants noxious GHG emissions may go down up to 35 % [15]. The second is related to brine discharge and its effect on the coastal marine ecosystem [16, 17].

It should be noticed that most of these studies are limited in scope, since they minimize either the cost of RO desalination or its environmental impact as unique criterion.

In practice, however, it is critical to quantify simultaneously their environmental and economic performance to fully assess the benefits of these technologies and to evaluate the effect of their integration with renewable energies. A mixed-integer nonlinear programming (MINLP) model was introduced by Vince et al. to assess for the first time both, the economic and environmental performance of this process [18]. This study did not consider the integration of RO with any renewable source of energy. Another multi-objective optimization approach was presented by Spyrou and Anagnostopoulus [19], who investigated the optimum design of a stand-alone desalination system powered by renewable energy sources and a pumped storage unit.

This work addresses the simultaneous optimization of the economic and environmental performance of RO systems integrated with solar thermal energy and thermal energy storage. We propose a mixed-integer nonlinear (MINLP) model, in which the environmental performance of the operation and construction is quantified via life cycle assessment (LCA) principles. This approach allows identifying the main sources of environmental impact considering the entire life cycle of the plant. Numerical results show that it is possible to obtain significant reductions in GHG emissions at a minor increase in cost by integrating RO with solar energy. The article is laid out as follows. The problem under study is formally introduced in section 2, while in section 3 we provide a brief description of the system. In section 4, the methodology and mathematical model are presented. Some numerical results are presented in section 5, and the conclusions are drawn in section 6.

2. Process description

The desalination system under study is given in Fig.1. It is composed of four subsystems, which are briefly explained below. Further details on the system can be found elsewhere [20].

2.1. Reverse Osmosis unit

The reverse osmosis unit is the equipment where the desalination process itself takes place. The process requires a standard RO unit with b trains, each one operated by one high pressure pump P_{RO}. Every train comprises *mod* pressure vessels which are arranged in arrays (2:1 or 4:2) that are connected in parallel. Typically, from 1 to 8 spiral-wound membranes are accommodated in series inside a pressure vessel. The pump supplies saline water to the membranes for filtration where salt is removed to obtain potable water. After this, the still pressurized brine is passed through a hydroturbine (H) to partially regain the energy and use it for the P_{RO} operation.

2.2. Solar Rankine Cycle unit

The Rankine cycle (RC) produces the electrical energy required by the high pressure pump of the reverse osmosis subsystem (RO). The working fluid of RC is water. In the boiler (B), the subcooled water is converted into superheated steam (6) by exchanging heat with the hot mineral oil of the solar-thermal subsystem. The superheated vapour is expanded in the turbine (turb) (7), generating electricity for P_{RO}. A small part of this electricity is used to operate the RC pump (P_{RC}). The humid vapour leaving the turbine passes through the condenser (cond), where it completely condensates (8) and then returns to the boiler.

2.3. Solar Thermal unit

The solar thermal unit provides heat to the boiler of the RC. Parabolic trough collectors (col) are employed to transfer solar energy to the heat mineral oil. A gas heater (GFH) is coupled with the solar collectors as a back up system in order to cope with the intermittent radiation and maintain the oil temperature constant. This oil is used in the boiler to generate steam.

2.4. Thermal Energy Storage

Thermal energy storage (TES) is integrated in the system to use the solar energy more efficiently. A molten-salt thermocline is considered. Molten salt is used as the heat transfer fluid (HTF) that transports thermal energy between the storage unit and the remaining parts of the power system (e.g., collector field and RC boiler) [21, 22].

3. Mathematical model

The optimization task is posed in mathematical terms as a mixed-integer nonlinear problem (MINLP). The model comprises the following sets of equations: equations for the RO, Rankine cycle and solar system, and objective function equations. A detailed description of the equations of the RO and Rankine cycle can be found elsewhere [20]. We focus here on describing the equations used to model the solar system that integrates the heat storage and as well as in the objective function calculations.

To model the heat storage system we use the following energy balance:

$$\overline{Q}(k,t) + \overline{Q}(k',t) + \overline{Q}(k'',t-1) = \overline{Q}(k''',t) + \overline{Q}(k'',t) \qquad (1)$$
$$k = col, k' = GFH, k'' = TES, k''' = B, \forall t$$

where $\overline{Q}(col,t)$ is the thermal energy captured by the collectors, $\overline{Q}(GFH,t)$ is the energy provided by the fossil fuel combusted in the GFH, $\overline{Q}(B,t)$ is the energy required by the RC boiler and $\overline{Q}(TES,t)$ is the thermal energy accumulated in the storage at the end of period t. The maximum amount of thermal energy that can be accumulated is given by the maximum storage capacity CAP:

$$\overline{Q}(TES,t) \leq CAP \qquad \forall t \qquad (2)$$

The solar energy absorbed by the solar collectors and converted into heat energy of thermal oil is calculated as follows, i.e.:

$$Q(k,t) = G(t)A(k)\eta(k,t) \qquad k = col, \forall t \tag{3}$$

Where $G(t)$ represents the solar radiation, which depends on the time period of the day and month. The daily solar irradiance (MJ/m^2 day) is extracted from [29]. The efficiency of the medium-high temperature parabolic trough collectors η_{col} is estimated as follows[30]:

$$\eta(k,t) = \eta_o(t) - a_1(T^{av}(t) - T^{amb}(t)) - a_2\left(\frac{T^{av}(t) - T^{amb}(t)}{G(t)}\right) - a_3 G(t)\left(\frac{T^{av}(t) - T^{amb}(t)}{G(t)}\right)^2 \tag{4}$$

$$k = col, \forall t$$

where η_0 is the collector optical efficiency, a_1, a_2, a_3 are coefficients, and $T^{amb}(t)$ is the ambient temperature in time period t. $T^{av}(t)$ is the average temperature in solar collector:

$$T^{av}(t) = \frac{T(i,t) + T(i',t)}{2} \qquad i = 11, i' = 12 \tag{5}$$

The heat produced by the combustion of natural gas in the heater is given by:

$$Q(k,t) = m_{NG}(t) \cdot LHV \cdot \eta(k) \qquad k = GFH \tag{6}$$

In this equation m_{NG}(t) is the mass flow rate of natural gas, LHV is the lower heating value of natural gas, and $\eta(GFH)$ is the thermal efficiency of the natural gas heater.

4. Objective functions and methodology

4.1. Economic evaluation: Specific total cost

The economic performance of the process is quantified through the unitary production cost per m^3 of water generated (continuous variable STC), which is defined as follows:

$$STC = \frac{Z}{M_d} \tag{7}$$

where Z is the total cost of the plant, and M_d is the total amount of water produced over the whole plant time span LT (in years). The latter term is calculated as follows:

$$M_d = \frac{3600 \cdot m(3) \cdot b \cdot LT \cdot H}{\rho(3)} \tag{8}$$

where H is number of working hours per year.

The total cost of the plant includes the investment and operation cost associated with the solar Rankine cycle SRC (RC with the solar thermal unit and TES) and the RO unit (Z_{SRC} and Z_{RO}, respectively):

$$Z = Z_{SRC} + Z_{RO} \tag{9}$$

The total cost of the SRC accounts for the capital investment cost of every unit of the system ($ICC(k)$) as well as the annual operating and maintenance cost ($COM(k)$). The total cost of the integrated facility accounts also for the cost of natural gas (C_{NG}) and electricity (C_{EL}) during the life time of the plant [20, 31].

$$Z_{SRC} = \sum_k AM \cdot (ICC(k) + COM(k)) \cdot LT + C_{NG} + C_{EL} + C_{TES} \tag{10}$$

$$k = col, turb, cond, B, P_{tf}, P_{RC}$$

where AM is the amortization factor evaluated as follows:

$$AM = \frac{int(1+int)^{LT}}{(1+int)^{LT}-1} \tag{11}$$

in this equation int represents the annual interest rate and LT is plant life span. The operating cost of the RO unit is determined as follows:

$$Z_{RO} = [1.4(CC_{swip} + CC_{P_{RO}} + CC_{mem} + CC_{mod})AM + COM_{RO}] \tag{12}$$

The coefficient 1.4 accounts for the indirect capital cost as well as the cost of the site. CC_{swip}, $CC_{P_{RO}}$, CC_{mem}, CC_{mod} are direct capital costs of seawater intake and pretreatment, RO pump, membrane elements and membrane modules. Details on the calculation of each term in equations 10 and 12 can be found in Appendix 1 of the supplementary material and in [20, 31] .

4.2. Environmental impact objective function

In our study we coupled multi-objective optimization with LCA principles. This approach was first proposed by Stefanis and Pistikopoulus [32], and formally described by Azapagic and Clift [33]. This combined approach has been applied to a wide variety of engineering problems of different nature such as the design and planning of supply chains [34–39], the synthesis of absorption cooling systems [40], and the superstructure optimization of chemical plants and biotechnological processes [41, 42], among others. Particularly, the environmental assessment of the RO plant is performed according to the CML 2001 methodology [43]. We consider the following sources of impact in the LCA analysis: construction (pumps, turbine, solar collector, modules, membranes , condenser, evaporator, boiler, TES) and operation (electricity and natural gas). The functional unit

taken as reference is 1 m^3 of final potable water collected at the outlet. The environmental metric to be optimized is the specific environmental impact (SEI), which quantifies the amount of GHG emissions per unit of water produced.

$$SEI = \frac{TGWP}{M_d} \tag{13}$$

where $TGWP$ denotes the total global warming emissions expressed in equivalent tons of CO_2. The value of this variable is determined from the GHG emissions and associated damage factors df(c). These damage factors quantify the GWP impact of the GHG emissions (measured in equivalent tons of CO_2), expressing them on a common basis.

$$TGWP = \sum_c TLCI(c) \cdot df(c) \tag{14}$$

The total amount of chemical c released to the environment is determined from the LCIs associated with the generation of natural gas and electricity and that associated with the construction phase:

$$TLCI(c) = LCI_{NG}(c) + LCI_{EL}(c) + LCI_{const}(c) \tag{15}$$

The life cycle inventory of emissions associated with the generation of natural gas and electricity are determined as follows:

$$LCI_{NG}(c) = \sum_t \frac{\omega_{NG}(c) Q(k,t) LT \cdot H}{\eta(k)} \qquad k = GFH, \forall c \tag{16}$$

$$LCI_{EL}(c) = \sum_t \frac{\omega_{EL}(c) W(k,t) LT \cdot H}{\eta(k)} \qquad k = P_{tf}, \forall c \tag{17}$$

Here, ω_{NG} and ω_{EL} denote the life cycle GWP emissions associated with the consumption of 1 kWh of electricity and 1 MJ of natural gas burned, respectively. These data are

available in environmental databases (Ecoinvent). The LCI of the construction denoted by $LCI_{const}(c)$ is calculated using the following equation:

$$LCI_{const}(c) = \sum_{k}(LCI(k,c)) + LCI(TES) + LCI_{mem} + LCI_{mod} \tag{18}$$

where the LCIs of equipment unit are determined as follows:

-Pumps and turbine:

$$LCI(k,c) = M(k) \cdot \omega_{Steel}(c) \qquad k = P_{tf}, P_{RC}, P_{RO}, turb, \forall c \tag{19}$$

where $M(k)$ is weight of equipment k, ω_{Steel} is the LCI associated with the production of 1 kg of stainless steel;

- Collector [47]:

$$LCI(k,c) = (Fg \cdot \omega_{FlatG}(c) + Rs \cdot \omega_{Reinf}(c)) \cdot A_{col}; \qquad k = col, \forall c \tag{20}$$

where Fg is the amount of flat glass used in parabolic trough collector per square metre of collector area (kg/m^2); Rs is the amount of reinforced steel used in the parabolic trough collector (kg/m^2) ; $\omega_{FlatG}(c)$ denotes the life cycle emissions per 1 kg of flat glass and $\omega_{Reinf}(c)$ represents the life cycle emissions per 1 kg of reinforced steel;

- Membranes :

$$LCI_{mem}(c) = n \cdot b \cdot A \cdot thick \cdot \rho_{amid} \cdot \omega_{Amid}(c) \qquad \forall c \tag{21}$$

where n is number of membranes per each RO train, b is number of trains, $thick$ is the membrane's thickness; ρ_{Amid} is the density of the polyamide and $\omega_{Amid}(c)$ represents the LCI emissions associated with the production of 1 kg of polyamide;

- Modules :

$$LCI_{mod}(c) = b \cdot mod \cdot Mmod \cdot \omega_{FGmod}(c) \qquad \forall c \tag{22}$$

where mod is number of pressure vessels per each train ,$Mmod$ is the weight of the pressure vessel and $\omega_{FGmod}(c)$ is the impact of 1 kg of fibre reinforced plastic ;

- Boiler, condenser and gas fired heater:

$$LCI(k,c) = A(k) \cdot s \cdot \rho_{steel} \cdot \omega_{Steel}(c) \qquad k = B, cond, GFH, \forall c \tag{23}$$

where $A(k)$ is heat transfer area, s is the thickness of the tubes in the heat exchangers and ρ_{steel} is the density of steel;

- Storage [46, 48]:

$$LCI_{TES}(c) = (\omega_{Molt}(c) \cdot Refmolt + \omega_{Reinf}(c) \cdot Reinf + \omega_{Reinf}(c) \cdot Refsteel + \tag{24}$$
$$\omega_{Foam}(c) \cdot Reffoam + \frac{\omega_{Conc}(c) \cdot Refconc}{\rho_{conc}} + \omega_{Brick}(c) \cdot Refbrick) \cdot MS/MSref$$
$$\forall c$$

where $\omega_{Molt}(c)$ represents the life cycle emissions associated with the production of 1 kg of molten salts(KNO_3); $Refmolt$ is the referential amount of molten salts in the storage; $Refreinf$ denotes the referential amount of carbon steel ; $\omega_{Reinf}(c)$ represents the LCI emissions associated with the production of 1 kg of reinforced steel; $Refsteel$ denotes the referential amount of reinforced steel; $\omega_{Foam}(c)$ represents the LCI emissions associated with the production of 1 kg of foam glass; $Reffoam(c)$ is the referential amount of foam glass; $\omega_{Conc}(c)$ denotes the LCI emissions associated with the production of 1 m_3 of concrete; $Refconc$ is the referential amount of concrete; rho_{conc} is the density of concrete; $\omega_{Brick}(c)$ represents the LCI emissions associated with the production of 1 kg of refractory brick; $Refbrick$ is the referential amount of refractory brick; MS denotes the weight of the

thermal mass and $MSref$ is the referential value of the thermal mass. The thermal mass consists of molten salts and silica sand. The weight of the thermal mass (MS) associated with the maximum thermal energy (CAP), is calculated as follows:

$$MS = CAP \cdot MSref / (\Delta T_{stor} \cdot (C_{ms} \cdot Refmolt + C_{sil} \cdot Refsil)); \tag{25}$$

where C_{ms} and C_{sil} are the specific heat of molten salts and silica sand respectively and ΔT_{stor} is the temperature difference between the top and bottom of the storage tank.

4.3. Solution procedure

The optimization task is expressed as a bi-criteria MINLP :

(M) $minU(x,y) = \{f_1(x), f_2(x)\}$

s.t. $h(x,y) = 0$

$g(x,y) \leq 0$

$x \in R, y \in \{0,1\}$

Here the functions f_1 and f_2 represent the economic and environmental performance of the system. Continuous variables x denote thermodynamic properties and operating conditions. Equations $h(x,y) = 0$ correspond to mass and energy balances, and thermodynamic properties estimation and cost and environmental impact calculations. Inequality constraints $g(x) \leq 0$ impose some bounds on the simulated variables. To solve this model, we employed the epsilon constraint method [44].

5. Case study

We illustrate the capabilities of our approach through the design of a RO facility located in Tarragona (Spain). The full details of the case study can be found in [20]. The parameters used in the model, environmental data and storage data are displayed in Tables 1, 2, 3. Further results of the calculations like properties of the flows,their temper-

atures, and energy load of the Rankine cycle, are given in the tables 4, 5, 6,7.

The thermal energy storage is an indirect system based on a thermocline tank with molten salt inside. This is a mixture of sodium and potassium nitrate (60% and 40%). Silica sand is used as filling material, acting as a primary storage material and making the storage system cheaper [46]. The capital cost of this system is 35 % lower than that of a two-tank storage system [21, 22]. The thermocline storage is operated with a temperature difference of 50 K between the top and bottom parts of the storage [5]. The environmental impact of the process was assessed via the CML 2001. The impact during the operation accounts for the impact of natural gas and electricity. The impact of the manufacture considers the high pressure pump, turbine, solar collector, storage, membranes, modules, condenser, boiler of the RC, and gas fired heater. Different construction materials were considered:

1. Pumps, turbine, hydroturbine, condenser, boiler, gas fired heater - stainless steel;

2. Membranes - cross linked fully aromatic polyamide composite;

3. Modules - FRP/fiberglass body, filament wound fiberglass reinforced epoxy tubing, end plugs PVC, end rings aluminum;

4. Solar collector - flat glass and reinforced steel

5. Storage - molten salts, carbon steel, reinforced steel, foam glass, concrete, refractory brick and silica.

The weights of the materials used in the parabolic trough collector and thermal energy storage, both required in the LCA calculations, were estimated from the literature [46–48]. The CO_2 emissions, associated with the production of each unit of material were retrieved from the Ecoinvent database V2.2.

The MINLP problem was coded in GAMS. Due to the small number of binary variables, it was possible to solve this MINLP by an exhaustive enumeration, that is, by solving NLPs for each possible combination of binaries. Each NLP was calculated using

CONOPT 3.14 [49]. The Pareto curve obtained after applying the ε - constraint method is depicted in Fig. 2, in which we have highlighted the two extreme solutions (i.e., designs A and B). Design A, which corresponds to the minimum STC design, does not contain collectors. In contrast, the minimum SEI design (design B) contains collectors with a total area equal to 146 000 m^2 and a storage capacity of 200 MWh. Note that adding collectors and heat storage in the system rises the cost from 0.88 to 1.01 €/m^3 (14 %), but at the same time it allows reducing the environmental impact from 4.08 to 1.81 kg CO_2/m^3 (55.6 %). As we move from the minimum STC solution, where no collectors are installed, towards the minimum SEI alternative, the model decides to increase the collectors area and storage capacity. In the same figure, we have depicted the points that result from optimizing the MINLP with a constraint that fixes the heat storage capacity to zero. As expected, these points lie entirely above the ones provided by the model when heat storage is allowed. This is because the use of heat storage improves the performance of the overall system, thereby reducing the total cost. Thus, heat storage makes the system more efficient, as it allows (with the same collectors area) increasing the solar fraction in the process and decreasing the natural gas consumption, which leads to less CO_2 emissions .

The dependence of the collectors' area and capacity of the storage on the specific environmental load is shown in Fig. 3. As we increase the collectors' area, we need more heat storage capacity, which leads to significant reductions in environmental impact. When the capacity of the storage reaches 30 MWh, which is the power required by the RC boiler, the slope of the curve CAP-SEI changes. This happens because the quantity of molten salts is relatively small at the beginning, but grows drastically as we increase the heat storage capacity, thereby increasing in turn the impact associated with their production.

The charging and discharging profiles of the storage and the main thermal energy flows during January (one of the months with lowest irradiance) and June (one of the months

with highest irradiance) are given in Fig. 4 and 5. The notation used here is as follows: $Q(col,t)$ is the thermal energy received by the collectors, $Q(GFH,t)$ is the energy generated from the natural gas combustion in the fired heater GFH, $Q(B,t)$ is the energy required by the RC boiler, and $Q(TES,t)$ is the thermal energy accumulated in the storage at the end of every period t. $Q_{colef}(t)$ is the total energy provided by the collectors and the TES to the boiler in each period t. The profile shows the behaviour of the storage during the operation. As seen, when the solar energy exceeds the demand (Q_{col} <Q_B), the excess of energy starts accumulating in the TES. When the energy from the solar collector falls below the level required by the RC boiler ($Q(col,t)$ <$Q(B,t)$), the TES starts discharging, so the system is fed with energy from the solar collectors and TES simultaneously. $Q_{colef}(t)$ represents the sum of solar energy coming from the collector and the TES feeding the RC boiler. In the absence of sunshine, and when TES cannot fully cover the demand, then the required energy is obtained from natural gas. When TES is completely discharged, only natural gas is employed. It's possible to see that within January TES is active within 14 hours (7 hours of charging, and 7 hours of discharging), whereas in June it operates 4 hours more (8 of charging and 10 of discharging).

In terms of total cost, in the minimum SEI case it is 14.0 % higher than in the minimum STC case, while the SEI is reduced by 55.6 % (Fig.6). This can be attributed to the fact that TES is incorporated in the system, thereby increasing the solar fraction. The amount of natural gas consumed and the corresponding environmental load is significantly lower. Particularly, it is possible to avoid 110 kton of CO_2 emissions to the atmosphere considering the entire plant life time, which is equivalent to the amount of yearly CO_2 emissions of countries like Macedonia or Mongolia. The cost data is shown in Table 8. The total cost in the case of min SEI is greater at the cost of collector plus TES and less the gas spared in this system. We can also see that in the min STC solution the largest expenditures are associated with the natural gas consumption, while in the min SEI design the solar

collectors represent a large percentage of the cost.

The results of the calculations for the environmental impact minimization are presented in Table 9. The CML 2001 method provides as output the impact expressed in equivalent kg of CO_2 emissions. The environmental impact of the construction is very small (around 9 %) in comparison with that coming from the operation, and can thus be neglected. This is consistent with other works in the literature [50]. It should be noticed that the impact of the manufacturing phase mainly comes from the TES. The key process characteristics for the extreme designs are given and compared with referential values in Table 10. The cost of electricity generated with the Rankine cycle varies from 15.4 Eurocents/kWh for the min STC design, to 18.9 Eurocents/kWh for the min SEI alternative. The minimum cost design (design A) does not contain any solar collectors, so no storage is involved and the annual solar fraction is zero. The min SEI design contains solar collectors with an area of 146 000 m^2 and a maximum storage capacity of 200 MWh. Particular attention should be given to the value of the solar fraction (the share of energy satisfied by solar energy). In design B, the storage allows reaching a 60 % of solar energy with a collectors area of 146 000 m^2. The specific total cost of the final water in this case is 1.01 €/m^3.In contrast, in the minimum cost design, the solar fraction is zero, since no collectors are installed.

6. Conclusions

This work addressed the design of reverse osmosis plants coupled with a thermal solar Rankine cycle. We presented a rigorous MINLP that identifies optimal process configurations in terms of the economic and environmental performance. The environmental performance was measured via the overall contribution to global warming,which was quantified using the CML 2001 methodology that implements LCA principles. The method was applied to a case study of a reverse osmosis plant coupled with a solar Rank-

ine cycle and a thermal energy storage located in Tarragona. It was shown that heat storage makes the process more efficient, leading for CO_2 emissions reductions of up to 55.6 % at the expense of a cost rise of 14 %. This study aims to facilitate the evaluation and comparison of more efficient technologies for energy generation that reduce the consumption of fossil fuels.

7. Nomenclature

Abbreviations

B	Boiler
col	Solar collector
cond	condenser
EL	Electricity
GFH	gas fired heater
LCA	Life Cycle Assessment
LCI	Life cycle inventory
NG	Natural gas
H	Hydroturbine
P	Pump
RC	Rankine cycle
RO	Reverse osmosis
SR	Solar rankine cycle
SEI	Specific environmental impact
STC	Specific total cost
turb	Turbine
TES	Thermal energy storage

Indices

C	Chemicals indexed by c
I	Streams indexed by i
K	Unit of the process indexed by k
T	Time period indexed by t

Subscripts

$colef$	Sum of energy coming from the collectors and thermal energy storage
$const$	Construction
hpp	High pressure pump
ins	Insurance
kwR	KW, produced in the Rankine Cycle
lab	Labour
mem	Membrane
mod	Pressure vessel
o	Optical
$swip$	Seawater intake and pretreatment
tf	Thermal fluid

Superscripts

av	Average
amb	Ambiental

Parameters

AM	Amortization factor
a_1	Collector constant 1
a_2	Collector constant 2
a_3	Collector constant 3
b	Number of RO trains
df	Damage factor
C_{ms}	Specific heat of the molten salts
C_{sil}	Specific heat of the silica sand
$G(t)$	Solar radiation in time period t
H	Hours per year
int	Annual interest rate
LHV	Calorific capacity (heating value)of natural gas
LT	Life time of the plant
$M(k)$	Weight of equipment k
$Mmod$	Weight of a pressure vessel
mod	Number of modules
n	Number of membranes
$Price_{EL}$	Price of electricity
$Price_{NG}$	Price of natural gas
$Price_{TES}$	Price of kWh of storage capacity
s	Thickness of the tubes in the heat exchangers
$thick$	Thickness of the membrane
$T^{amb}(t)$	Ambient temperature in period t
ΔT_{stor}	Temperature difference between top and bottom parts of the storage tank
$\eta(k)$	Efficiency of unit k
$\omega_(c)$	Life cycle GWP emissions
ρ	Density

Variables

A	Area, m^2
C	Cost, €
CAP	Capacity of storage, kWh
CC	Capital cost , €
ICC	Investment capital cost,€
$COM(k)$	Operation and maintenance cost of the unit €/year
LCI	Life cycle impact assessment associated with fuel, kg CO_2 eq]$\times 10^6$ (million kg)
$m(i)$	Mass flow rate of the stream i, kg/s
M_d	Volume of permeated water through life time of the plant, m^3
MS	Weight of the thermal mass (molten salts and silica), kg
$Q(k)$	Thermal power of unit k, kW
$\overline{Q}(k,t)$	Thermal energy of unit k in period t, kWh
SEI	Specific total impact, kg CO_2eq/m^3
STC	Specific total cost, €/m^3
T	Temperature , K
$TGWP$	Total global warming emissions,kg CO_2eq
$TLCI$	Total amount of chemical c released to the environment, kg
Z	Total investment and operation cost, €
ΔP	Transmembrane pressure, Pa

References

[1] L. Greenlee, D. Lawler, B. Freeman, B. Marrot, P. Moulin, Reverse osmosis desalination: Water sources, technology, and today's challenges , Water Research 43 (9) (2009) 2317–2348 .

[2] Y. Kim, S. J. Kim, Y. S. Kim, S. Lee, I. S. Kim, J. Kim, Overview of systems engineering approaches for a large-scale seawater desalination plant with a reverse osmosis network, Desalination 238 (1–3) (2009) 312–332.

[3] P. Arce, M. Medrano, A. Gil, E. Oró, L. Cabeza, Overview of thermal energy storage (tes) potential energy savings and climate change mitigation in spain and europe, Applied Energy 88 (8) (2011) 2764–2774.

[4] U. Herrmann, Thermal storage concept for a 50 mw trough power plant in spain, Tech. rep., FLAGSOL (2006).

[5] J. Pacheco, S. William, J. Kolb, Development of a molten-salt thermocline thermal storage system for parabolic trough plants, Journal of solar energy engineering 124 (2002) 1–6.

[6] V. Hassani, H. Price, Modular trough power plants, Solar Engineering (2001) 437–444.

[7] C. Charcosset, A review of membrane processes and renewable energies for desalination, Desalination 245 (1-3) (2009) 214–231.

[8] A. R. Bartman, A. Zhu, P. D. Christofides, Y. Cohen, Minimizing energy consumption in reverse osmosis membrane desalination using optimization- based control, Journal of Process Control 20 (10) (2010) 1261–1269.

[9] Kaghazchi, T. and Mehri, M. and Ravanchi, M. T. and Kargari, A., A mathematical modeling of two industrial seawater desalination plants in the Persian Gulf region, Desalination 252 (1–3) (2010) 135–142.

[10] E. Koutroulis, D. Kolokotsa, Design optimization of desalination systems power-supplied by pv and w/g energy sources, Desalination 258 (1–3) (2010) 171–181.

[11] D. Voivontas, K. Misirlis, E. Manoli, G. Arampatzis, D. Assimacopoulos, A tool for the design of desalination plants powered by renewable energies, Desalination 133 (2) (2001) 175–198.

[12] A. Nafey, M. Sharaf, L. Garcia-Rodriguez, Thermo-economic analysis of a combined solar organic Rankine cycle-reverse osmosis desalination process with different energy recovery configurations, Desalination 261 (1-2) (2010) 138–147.

[13] H. Ben Bacha, T. Dammak, A. A. Ben Abdalah, A. Y. Maalej, H. Ben Dhia, Desalination unit coupled with solar collectors and a storage tank: modelling and simulation, Desalination 206 (1–3) (2007) 341–

352.

[14] W. Biswas, Life cycle assessment of seawater desalinization in western australia, World Academy of Science, Engineering and Technology 56 (2009) 369–375.

[15] R. Raluy, L. Serra, J. Uche, Life cycle assessment of desalination technologies integrated with renewable energies, Desalination 183 (2005) 81–93.

[16] D. Roberts, E. L. Johnston, N. A. Knott, Impacts of desalination plant discharges on the marine environment: A critical review of published studies , Water Research 44 (18) (2010) 5117–5128.

[17] Voutchkov, N., Overview of seawater concentrate disposal alternatives , Desalination 273 (2011) 205–219.

[18] E. Vince, F.and Aoustin, P. Brï£¡ant, F. Marechal, Lca tool for the environmental evaluation of potable water production, Desalination 220 (1–3) (2008) 37–56.

[19] I. Spyrou, J. Anagnostopoulos, Design study of a stand-alone desalination system powered by renewable energy sources and a pumped storage unit, Desalination 257 (1–3) (2010) 137–149.

[20] R. Salcedo, E. Antipova, D. Boer, L. Jiménez, G. Guillén-Gosálbez, Multi-objective optimization of solar rankine cycles coupled with reverse osmosis desalination considering economic and life cycle environmental concerns, Desalination.

[21] S. Flueckiger, Z. Yang, S. Garimella, An integrated thermal and mechanical investigation of molten-salt thermocline energy storage, Applied Energy.

[22] A. Gil, M. Medrano, I. Martorell, A. Lázaro, P. Dolado, B. Zalba, L. Cabeza, State of the art on high temperature thermal energy storage for power generation. part 1 —concepts, materials and modellization, Renewable and Sustainable Energy Reviews 14 (1) (2010) 31–55.

[23] J. Duffie, W. Beckman, Solar engineering of thermal processes, NASA STI/Recon Technical Report A 81.

[24] F. Vince, F. Marechal, E. Aoustin, P. Breant, Multi-objective optimization of RO desalination plants, Desalination 222 (1-3) (2008) 96–118.

[25] Fernandez-Sempere, J. and Ruiz-Bevia, F. and Garcia-Algado, P. and Salcedo-Diaz, R., Experimental study of concentration polarization in a crossflow reverse osmosis system using Digital Holographic Interferometry, Desalination 257 (1-3) (2010) 36–45.

[26] Y. Lu, Y. Hu, X. Zhang, L. Wu, Q.-Z. Liu, Optimum design of reverse osmosis system under different feed concentration and product specification, Journal of Membrane Science 287 (2) (2007) 219–229.

[27] D. F. Fletcher, D. E. Wiley, A computational fluids dynamics study of buoyancy effects in reverse

osmosis, Journal of Membrane Science 245 (1–2) (2004) 175–181.

[28] L. T. Biegler, I. Grossmann, A. Westerberg, Systematic methods of chemical process design, Prentice Hall, 1997.

[29] Generalitat de Catalunya Departament d'Indùstria, Comerç i Turisme, Atlas de radiacio solar a Catalunya (2000).

[30] J. Carles Bruno, J. Lopez-Villada, E. Letelier, S. Romera, A. Coronas, Modelling and optimisation of solar organic rankine cycle engines for reverse osmosis desalination, Applied Thermal Engineering 28 (17–18) (2008) 2212–2226.

[31] A. Nafey, M. Sharaf, Combined solar organic Rankine cycle with reverse osmosis desalination process: Energy, exergy, and cost evaluations, Renewable Energy 35 (11) (2010) 2571–2580.

[32] S. Stefanis, A. Buxton, A. Livingston, E. Pistikopoulos, A methodology for environmental impact minimization: Solvent design and reaction path synthesis issues, Computers & Chemical Engineering 20 (1996) 1419–1424.

[33] A. Azapagic, R. Clift, The application of life cycle assessment to process optimisation, Computers and Chemical Engineering 23 (10) (1999) 1509–1526.

[34] L. Puigjaner, G. Guillén-Gosálbez, Towards an integrated framework for supply chain management in the batch chemical process industry, Computers and Chemical Engineering 32 (4–5) (2008) 650–670.

[35] A. Hugo, E. Pistikopoulos, Environmentally conscious long-range planning and design of supply chain networks, Journal of Cleaner Production 13 (15) (2005) 1428–1448.

[36] I. Grossmann, G. Guillén-Gosálbez, Scope for the application of mathematical programming techniques in the synthesis and planning of sustainable processes, Computers & Chemical Engineering 34 (9) (2010) 1365–1376.

[37] G. Guillén-Gosálbez, I. Grossmann, Optimal design and planning of sustainable chemical supply chains under uncertainty, AIChE Journal 55 (1) (2009) 99–121.

[38] F. Mele, G. Guillén, A. Espuña, L. Puigjaner, An agent-based approach for supply chain retrofitting under uncertainty, Computers & Chemical Engineering 31 (5–6) (2007) 722–735.

[39] F. Mele, G. Guillén, A. Espuña, L. Puigjaner, A simulation-based optimization framework for parameter optimization of supply-chain networks, Industrial & Engineering Chemistry Research 45 (9) (2006) 3133–3148.

[40] B. Gebreslassie, G. Guillén-Gosálbez, L. Jimenez, D. Boer, A systematic tool for the minimization of the life cycle impact of solar assisted absorption cooling systems, Energy 35 (9) (2010) 3849–3862.

[41] R. Brunet, G. Guillén-Gosálbez, L. Jimenez-Esteller, Cleaner design of single-product biotechnological facilities through the integration of process simulation, multi-objective optimization, lca and principal component analysis, Industrial & Engineering Chemistry Research.

[42] G. Guillén-Gosálbez, J. Caballero, L. Jiménez, Application of life cycle assessment to the structural optimization of process flowsheets, Industrial & Engineering Chemistry Research 47 (3) (2008) 777–789.

[43] H. Althaus, C. Bauer, G. Doka, R. Dones, R. Hischier, S. Hellweg, S. Humbert, T. Köllner, Y. Loerincik, M. Margni, T. Nemecek, Implementation of life cycle impact assessment methods, Tech. rep., Swiss Centre for Life Cycle Inventories (December 2007).

[44] Y. Haimes, L. Lasdon, D. Wismer, On a bicriterion formulation of the problems of integrated system identification and system optimization, IEEE Transactions on Systems, Man, and Cybernetics 1 (3) (1971) 296–297.

[45] S. Kalogirou, Use of parabolic trough solar energy collectors for sea-water desalination, Applied Energy 60 (2) (1998) 65–88.

[46] National Renewable Energy Laboratory, Life Cycle Assessment of Thermal Energy Storage: Two-Tank Indirect and Thermocline.

[47] F. Küsgen, D. Kueser, Fresnel csp: a startling technology for solar generation, Power Engineering International.

[48] P. Viebahn, S. Kronshage, F. Trieb, Y. Lechon, Final report on technical data, costs, and life cycle inventories of solar thermal power plants, Tech. Rep. 502687, DLR CIEMAT (2008).

[49] A. Drud, A. CONOPT, A system for large scale nonlinear optimization, Tutorial for CONOPT Subroutine Library, ARKI Consulting and Development A/S, Bagsvaerd, Denmark.

[50] R. Raluy, L. Serra, J. Uche, Life cycle assessment of desalination technologies integrated with renewable energies, Desalination 183 (1–3) (2005) 81–93.

[51] P. S. I. GmbH, Survey of thermal storage for parabolic trough power plants, Tech. Rep. NREL/SR-550-27925, National Renewable Energy Laboratory, Cologne, Germany (September 2000).

List of Tables

Table 1: **Parameters used in the mathematical model**

Simbol	Definition	Value	Units
AM	Amortization factor	0.08	-
a_1	Collector constant 1	$4.5 \cdot 10^{-6}$	$1/K$
a_2	Collector constant 2	0.039	$W/(m^2K)$
a_3	Collector constant 3	$3 \cdot 10^{-4}$	$W^2/(m^2K^2)$
b	Number of RO trains	7	-
$(C_{ms}$	Specific heat of the molten salts	2.620	$kJ/(kg \cdot K)$
Cp_{sil}	Specific heat of the silicate	0.83	$kJ/(kg \cdot K)$
H	Hours per year	8760	h
int	Annual interest rate	0.05	-
LT	Life time of the plant	20	years
$M(P_{RC})$	Weight of the RC pump	1000	kg
$M(P_{RO})$	Weight of the RO pump	2000	kg
$M(P_{tf})$	Weight of the thermal fluid pump	500	kg
$M(turb)$	Weight of the turbine	30000	kg
LHV	Calorific capacity (heating value)of natural gas	47100	kJ/kg
$Mmod$	Weight of a pressure vessel	168	kg
mod	Number of the modules	100	-
n	Number of the membranes in each train	600	-
$Price_{EL}$	Price of the electricity	0.1082 €/kWh	
$Price_{NG}$	Price of the natural gas	0.0301 €/kWh	
$Price_{TES}$	Price of the kWh storage capacity	40	€
s	Thickness of the tubes in the heat exchangers	0.003	m
$thick$	Thickness of the membrane	$1.0 \cdot 10^{-6}$	m
ΔT_{stor}	Temperature difference between the top and the bottom parts of the storage tank	50	K
η_0	Collector optical efficiency	0.75	
$\eta(GFH)$	Thermal efficiency of the gas fired heater	0.75	-
$\eta(H)$	Hydroturbine efficiency	0.75	
$\eta(P_{RO})$	RO pump efficiency	0.75	-
$\eta(P_{RC})$	RC pump efficiency	0.6	-
$\eta(P_{tf})$	Pump efficiency of TF pump	0.6	-
$\eta(turb)$	Isentropic efficiency in the turbine	0.72	-
ρ_{Amid}	Density of the polyamide	1180	kg/m^3
ρ_{conc}	Density of the concrete	2400	kg/m^3
ρ_{NG}	Density of the natural gas	0.78	kg/m^3
ρ_{tf}	Density of the thermal fluid	753	kg/m^3
ρ_{steel}	Density of the steel	7800	kg/m^3

Table 2: **Individual environmental impact of construction materials**

Parameter	Material	Ecoinvent points
ω_{Amid}	Cross Linked fully aromatic polyamide composite [kg] (# 1815)	8.7015
ω_{Brick}	Refractory, basic, packed, at plant, [kg] (# 497))	2.3137
ω_{Conc}	Poor concrete, [m^3] (# 511)	123.07
ω_{EL}	Electricity, [kWh] (# 674)	0.50682
ω_{FlatG}	Flat glass, coated, at plant, [kg] (# 805))	0.66494
ω_{Foam}	Foam glass, at plant, [kg] (# 7160)	1.5683
ω_{FGmod}	Glass fibre reinforced plastic, polyester resin, hand lay-up, at plant, [kg](# 1816)	4.8911
ω_{Molt}	Potassium nitrate, as N, at regional storehouse, [kg] (# 52)	16.108
ω_{NG}	Natural gas, [MJ] (# 1363)	0.067927
ω_{Reinf}	Reinforcing steel, at plant, [kg] (# 1141))	1.4854
ω_{Steel}	Stainless steel 18/8, at plant, [kg] (# 1072)	5.2536

Table 3: **Referential values for construction materials used in storage ([46, 48])**

Parameter	Material	Amount, kg
FG	flat glass per 1 $m^2$of area of solar collector	18
$MSref$	thermal mass	1.79E+07
$Refmolt$	molten salts in the storage	7.68E+06
$Refreinf$	carbon steel	5.90E+05
$Refsteel$	reinforced steel	1.82E+05
$Reffoam$	foam glass	4.40E+04
$Refconc$	concrete	3.36E+06
$Refbrick$	refractory brick	4.32E+05
RS	reinforced steel	11

Table 4: **Physical and thermodynamic properties of the reverse osmosis streams**

Variable		Stream(i)				
		1	2	3	4	5
m(i)	flow rate , kg/s	88.89	188.89	85	103.89	103.89
X(salt,i)	concentration of salt	0.035	0.035	1.00E-04	0.064	0.064
$\rho(i)$	density, kg/m^3	1021.39	1021.39	997.17	1041.21	1041.21
$\mu(i)$	viscosity, Pa·s	9.41e-04	9.41e-04	8.90e-04	9.82e-04	9.82e-04
k_{mass}	mass transfer coefficient, m/s	1.00e-06	2.80e-05	1.59e-05	1.74e-05	1.74e-05
Re(i)	Reynolds number	140.04	140.04	66.60	73.78	73.78
Sc(i)	Schmidt number	635.54	635.54	615.94	650.90	650.90

Table 5: **Characteristics of the Rankine cycle streams**

Variable		RC stream			
		6	7	8	9
T(i)	temperature thermodynamic states, K	646.15	319.66	319.66	319.66
T_{sat}(i)	saturation temperature, K	531.51	319.66	319.66	531.51
P(i)	pressure, Pa	4424.17	10	10	4424.17
h(i)	enthalpy at thermodynamic state i, kJ/kg	3141.43	2397.06	198.85	204.14

Table 6: **Results of the calculation for the Rankine cycle**

	Variable	Value
m_{RC}	mass flow Rankine cycle, kg/s	10.31
A_{Cond}	area of condenser, m^2	1403.19
η_{RC}	thermal efficiency of Rankine cycle	0.25
Q_B	evaporation energy, kW	30276.43
Q_{Cond}	energy in condenser, kW	22658.27
W_{turb}	mechanical power in turbine, kW	7672.76
$W_{P_{RC}}$	mechanical power in RC pump, kW	91

Table 7: **Results of the calculation for the reverse osmosis unit**

	Variable	Value
W_{net}	net energy required by the RO system, kW	7581.76
RR	membrane recovery ratio (product-feed relation)	0.45
c_w	wall mass fraction	0.04
J_w	volumetric permeate flow rate, $m^3/(m^2s)$	3.84e-06
ΔP	transmembrane pressure, Pa	6.31e+06
W_{hpp}	energy required by pump, kW	1555.04
W_H	energy recovered by hydroturbine, kW	471.94

Table 8: **Cost of different units of the system for the system with storage (Pareto 2)**

Unit	Min SEI, million €	Min STC, million €
Total cost	357.6	280.2
Reverse osmosis unit	127.2	127.2
Solar Rankine cycle	230.3	153.0
Storage	7.2	0.0
Natural gas	40.6	99.3
Solar collectors	150.6	0.0

Table 9: **Environmental impact**

	min SEI [kg CO_2]	min STC [kg CO_2]
Operation	632,132,278	1,533,880,688
electricity	7,846,388	7,846,388
natural gas	624,285,890	1,526,034,300
Manufacture	58,295,590	1,130,526
Pump	18,390	18,390
Turbine	157,610	157,608
Collectors	4,970,920	0
Storage	52,194,150	0
Membranes	1,596	1,596
Modules	575,193	575,193
Condenser	56,350	56,350
Boiler	172,501	172,501
Gas fired heater	148,880	148,888
Total	690,427,868	1,535,011,214

Table 10: **Key process characteristics**

Characteristic	Design A	Design B	Referential value
collectors area, m^2	0	146000	-
Cost of energy from solar Rankine cycle, Eurocents/kWh	15.4	18.9	12-24
Electrical energy consumption (SPC), kWh/m^3	3.53	3.53	3-5.5
Environmental Impact (SPECO), kg CO_2 eq/m^3	4.08	1.82	3
Solar fraction, %	0	60	50
Specific total cost (STC), euro/m^3	0.88	1.01	0.9-1.3
Storage capacity (CAP), MWh	0	200	-

List of Figures

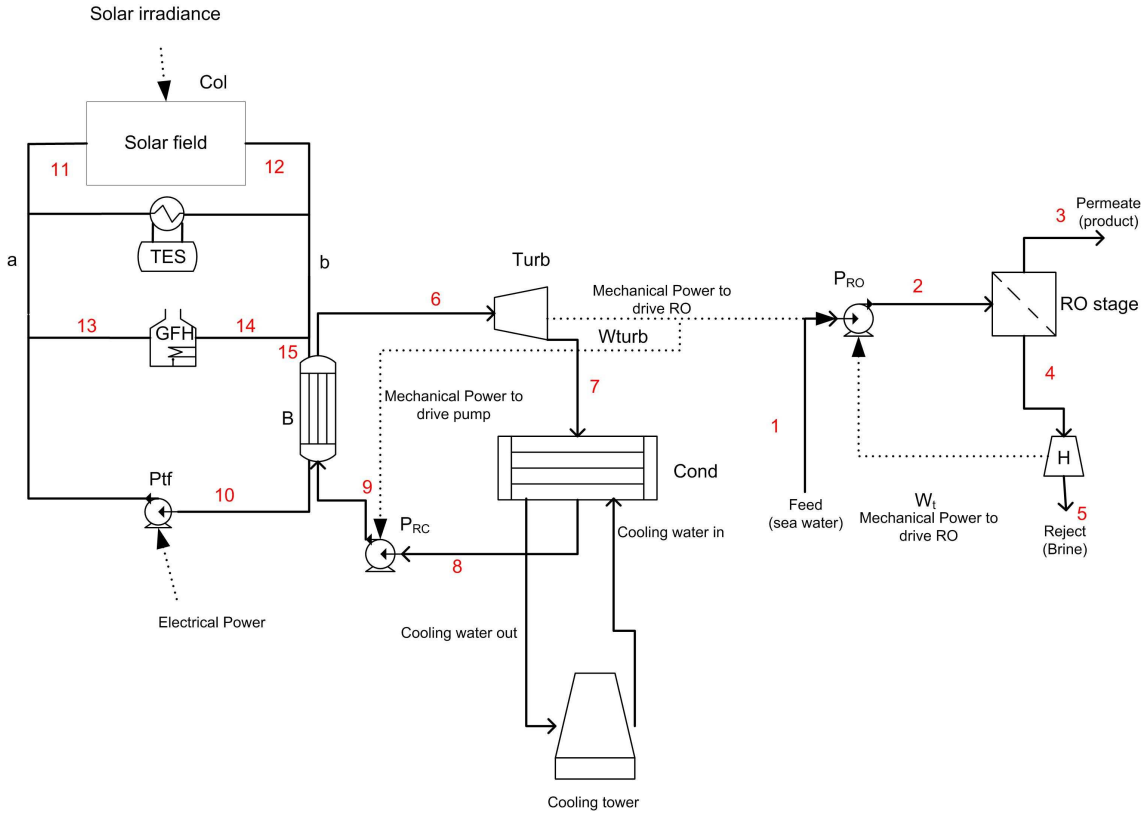

Figure 1: **Scheme of the process**

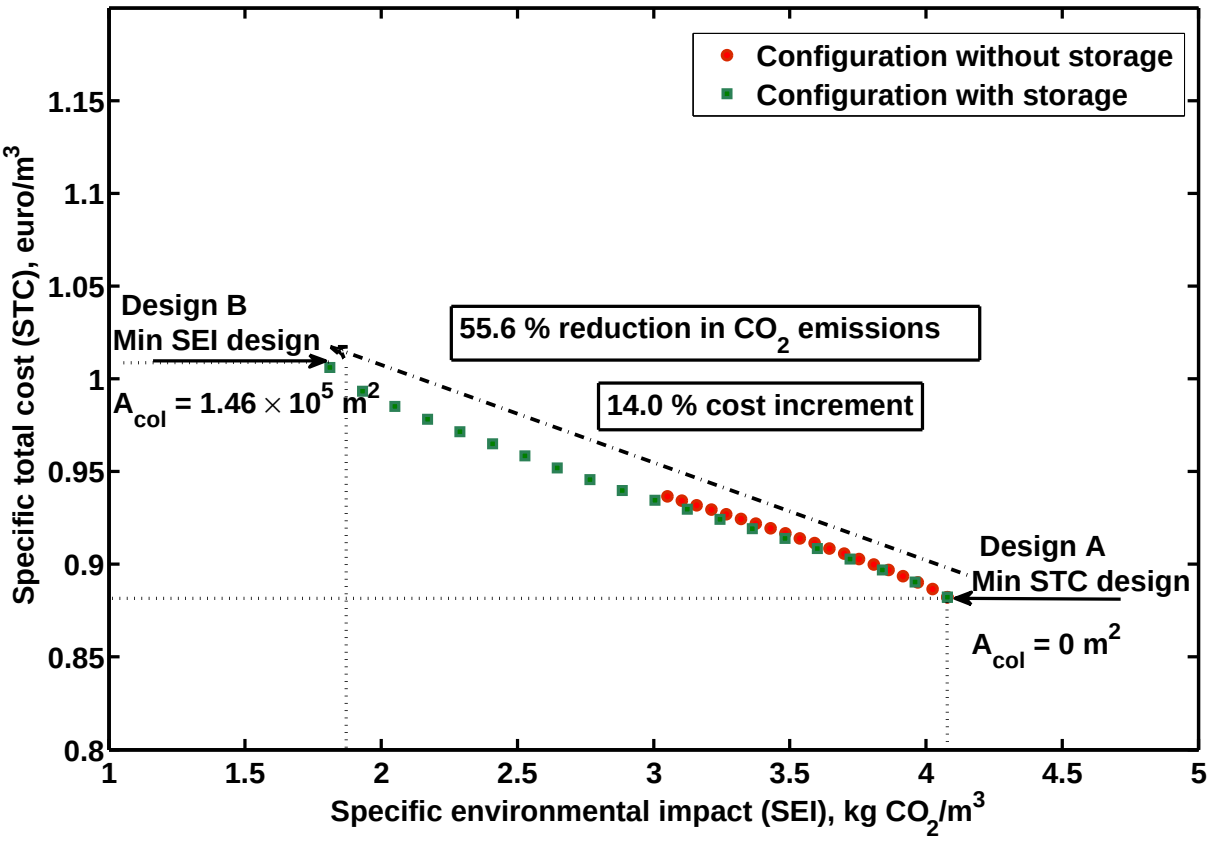

Figure 2: **Pareto set of optimal solutions**

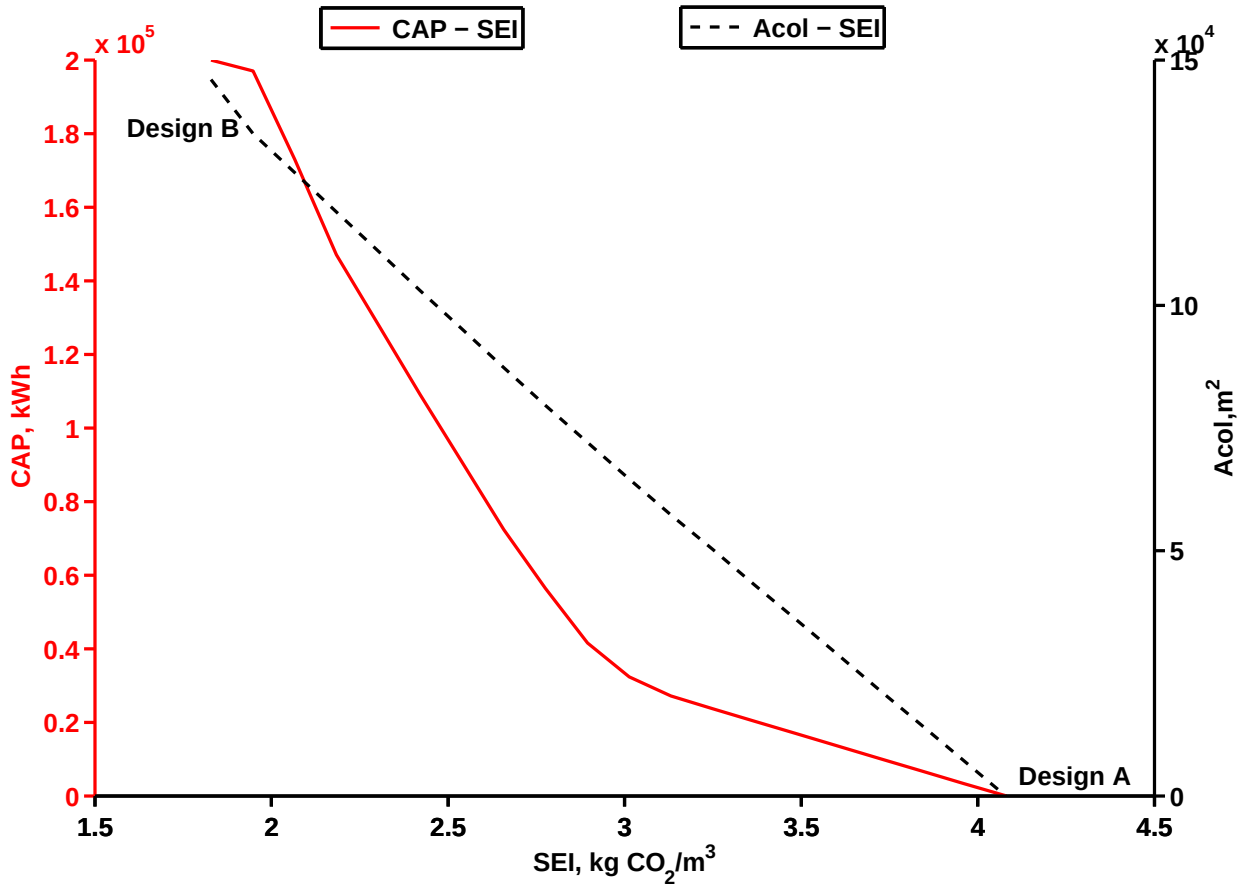

Figure 3: **Dependence of the collectors' area and capacity of the storage on the specific environmental load**

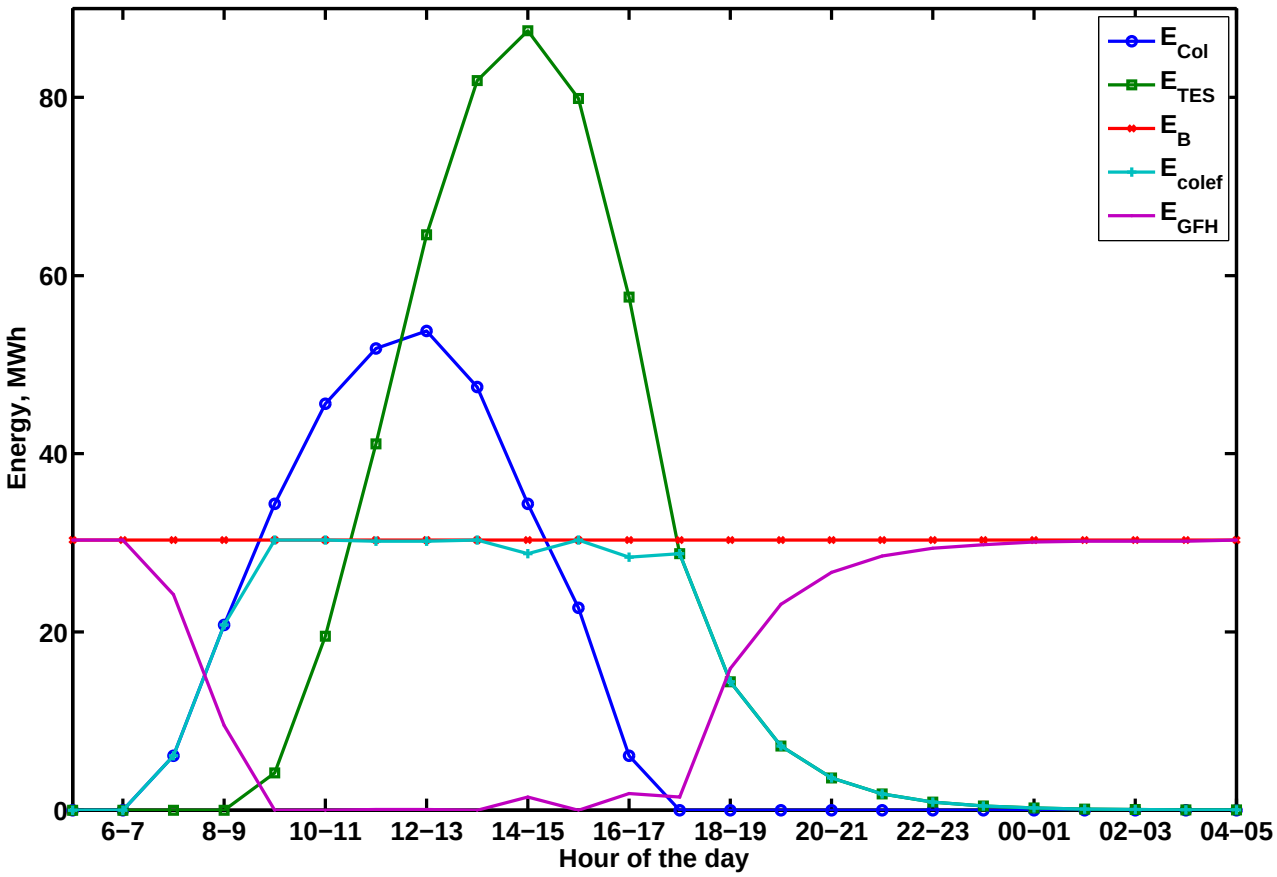

Figure 4: **Energy flows and charging and discharging profile of the TES in January for design B**

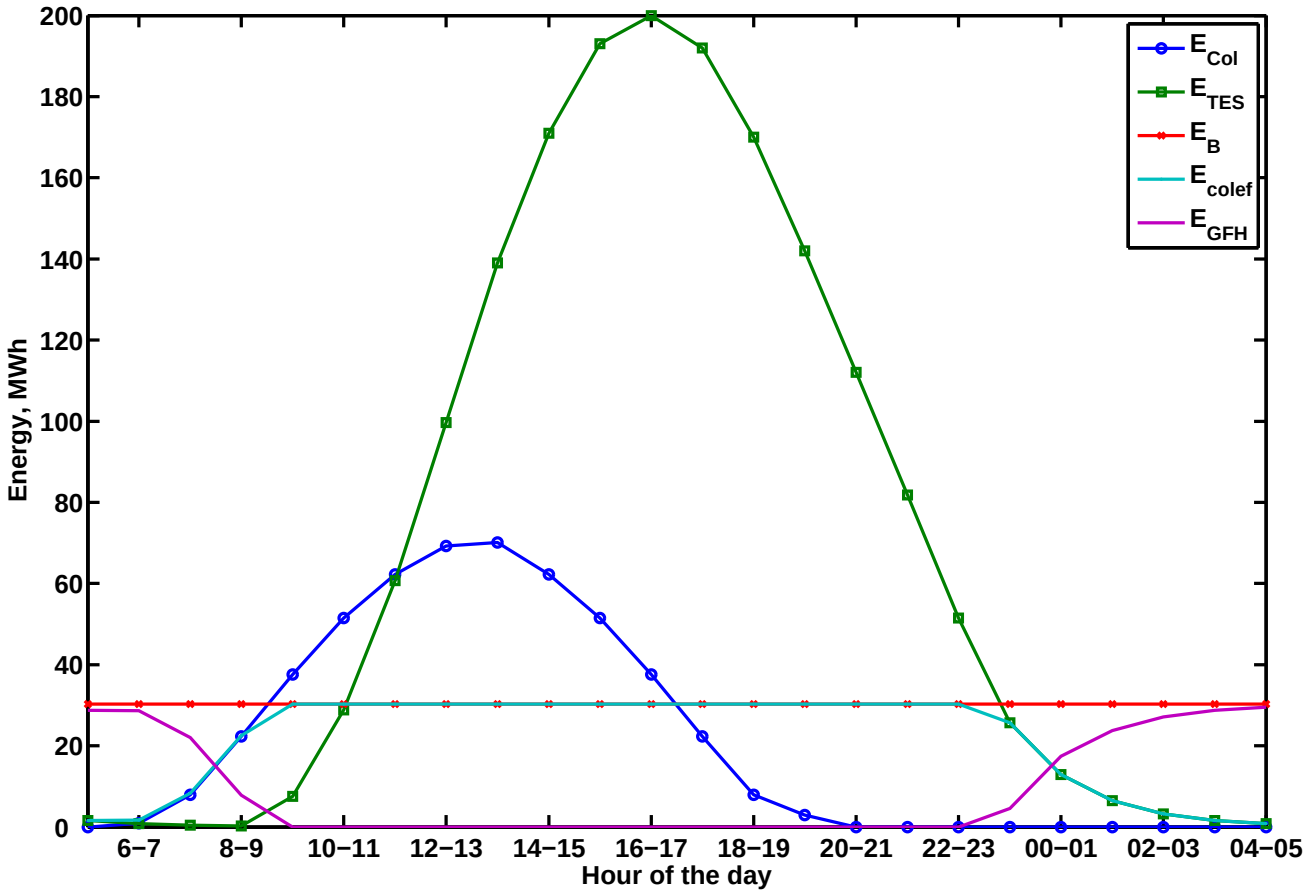

Figure 5: **Energy flows and charging and discharging profile of the TES in June for design B**

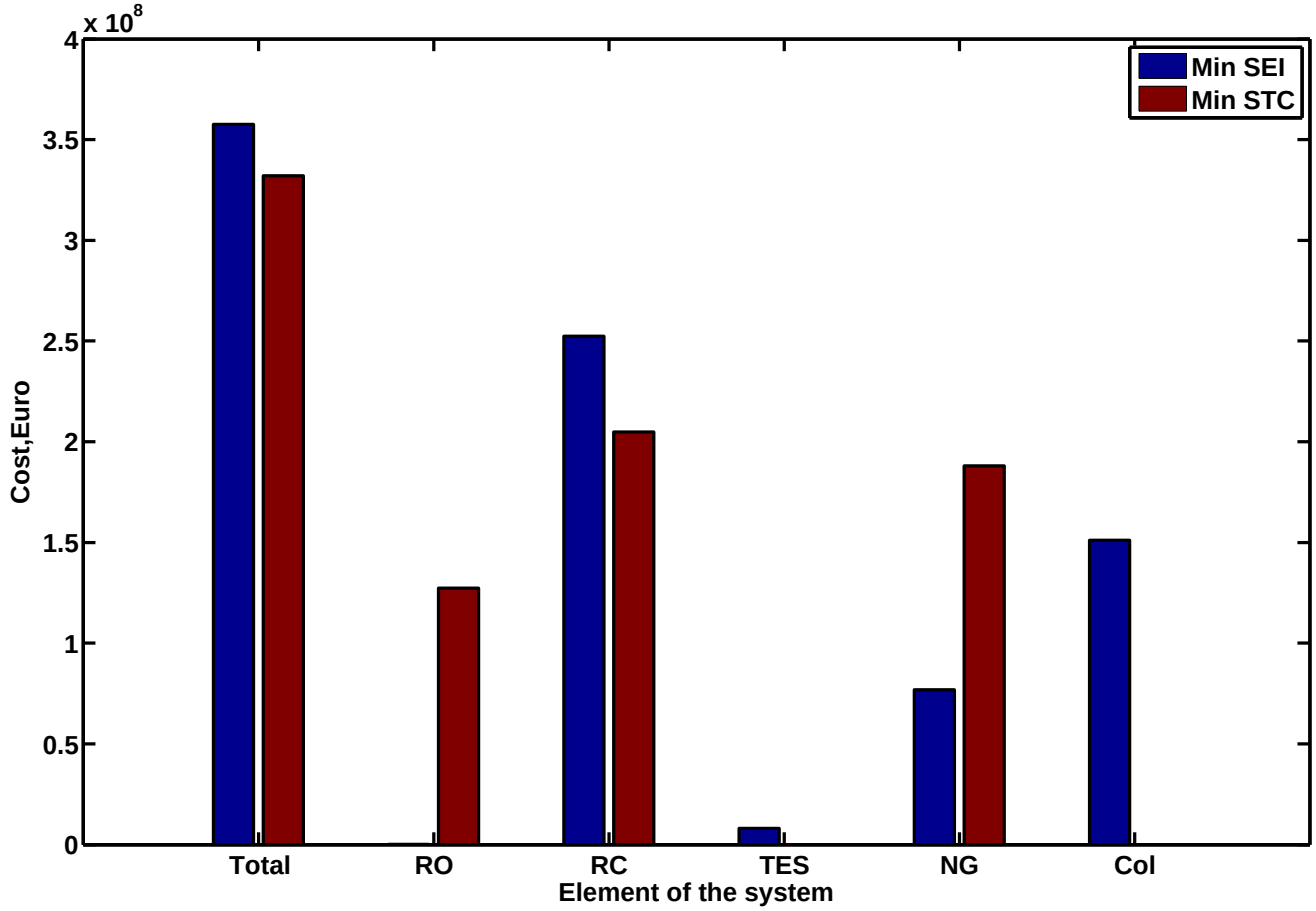

Figure 6: **Breakdown of the total cost**

Appendix 1. Cost estimation.The cost associated with the natural gas and electricity consumption is calculated as follows:

$$C_{NG} = Price_{NG} \cdot \frac{Q(k) \cdot LT \cdot H}{\eta(k)} \qquad k = GFH \tag{26}$$

$$C_{EL} = Price_{EL} \cdot \frac{W(k) \cdot LT \cdot H}{\eta(k)} \qquad k = P_{tf} \tag{27}$$

The cost of the TES is given by:

$$C_{TES} = Price_{TES} \cdot CAP \tag{28}$$

Where $Price_{TES}$ is the cost per unit of thermal energy delivered [51]. The cost per kWh of electricity produced in the turbine of the Rankine cycle (C_{KwR}) is obtained from:

$$C_{KwR} = \frac{Z_{SRC}}{W_{RC} \cdot LT \cdot H} \tag{29}$$

The total cost of the RO unit includes the capital cost associated with the seawater intake system (CC_{swip}), high pressure pumps $(CC_{P_{RO}})$, membranes (CC_{mem}), pressure vessels (CC_{mod}), as well as the operation and maintenance costs (COM_{RO}) related to the technical support required to ensure normal operating conditions. These terms are determined as follows:

$$CC_{swip} = 996 M_d^{0.8} \tag{30}$$

$$CC_{P_{RO}} = 393000 + 10710 \Delta P \tag{31}$$

$$CC_{mem} = Fe \cdot n \cdot P_{mem} \tag{32}$$

$$CC_{mod} = mod \cdot C_{mod} \tag{33}$$

where P_{mem} is the membrane price and C_{mod} is the pressure vessel price.

The operating cost of the RO unit accounts for the power used (COM_{power}), labor (COM_{lab}), chemicals (COM_{chem}), insurance (COM_{ins}), and membrane service (COM_{mem}).

$$COM_{RO} = COM_{power} + COM_{lab} + COM_{chem} + COM_{ins} + COM_{mem} \tag{34}$$

Details on these calculations can be found in [20].